Natural spleen cell ligandome in transporter antigen processing (TAP)-deficient mice

Elena Lorente [1,#], Concepción Palomo [1,#], Eilon Barnea [2], Carmen Mir [1], Margarita del Val [3], Arie Admon [2], and Daniel López [1,*]

[1] Unidad de Presentación y Regulación Inmunes, Instituto de Salud Carlos III, 28220 Majadahonda (Madrid), Spain.

[2] Department of Biology, Technion-Israel Institute of Technology, 32000 Haifa, Israel.

[3] Centro de Biología Molecular Severo Ochoa, Consejo Superior de Investigaciones Científicas (CSIC), 28049 Madrid, Spain.

[#] Equal contribution

*** Correspondence:** Dr. Daniel López. Unidad de Presentación y Regulación Inmunes. Centro Nacional de Microbiología. Instituto de Salud Carlos III. 28220 Majadahonda (Madrid), Spain. Tel: +34 91 822 37 08, FAX: +34 91 509 79 19, E-mail: dlopez@isciii.es

ABSTRACT

Peptides generated by proteases in the cytosol must be translocated to endoplasmic reticulum lumen by the transporter associated with antigen processing (TAP) prior to their assembly with major histocompatibility complex (MHC) class I molecules. Non-functional TAP complexes produce a drastic decrease of the MHC class I/peptide complexes presented on the cell surface. Previously, the cellular MHC class I ligandome from TAP-deficient cell lines was determined, but similar analysis from normal tissues remains open. Using high-throughput mass spectrometry to analyze the MHC-bound peptide pools isolated from ex vivo spleen cells of TAP-deficient mice, we identified 210 TAP-independent ligands naturally presented by murine MHC class I molecules. This ligandome showed increased peptide lengths, presence of multiple nested set peptides, and low theoretical MHC binding affinity. The gene ontology enrichment analysis of parental proteins of this TAP-independent sub-ligandome showed almost exclusively enrichment in tissue-specific biological processes related with the immune system as would be expected. Also, cellular components of the extracellular space (namely proteins outside the cell, but still within the organism excluding the extracellular matrix) were specifically associated with TAP-independent antigen processing from these ex vivo mice cells. In addition, functional protein association network analysis revealed low protein-protein interactions between parental proteins from TAP-independent ligandome. Finally, predominant endoproteolytic peptidase specificity for Leu/Phe residues in the P_1 position of the scissile bond at both ligand termini was found for the ex vivo TAP-independent ligands. These data indicate that the TAP-independent ligandome from ex vivo cells derives from a more diverse collection both of endoprotease activities and parental proteins, and where the cell origin and the contribution of extracellular environment are more relevant than in its equivalent cell lines.

Keywords: antigen presentation, immunodeficiency, mass spectrometry, MHC, TAP.

INTRODUCTION

The cytosolic proteases, among which stands out the proteasome, continuously degrade misfolded or prematurely terminated proteins, also named defective ribosomal products, as well as mature proteins with normal turnover kinetics. This proteolysis generates short peptides, some of which are transported into the endoplasmic reticulum (ER) lumen by the transporter associated with antigen processing (TAP) [1]. These peptides are assembled with de novo β2-microglobulin and MHC class I heavy chain to generate trimolecular stable MHC-I/peptide complexes that are exported to the cell membrane and exposed to cytotoxic $CD8^+$ T lymphocyte recognition (reviewed in [2] [3]). This classical antigen presentation pathway is the key element in the adaptive immune response against viruses and tumors [4, 5].

The TAP deficiency syndrome, a rare condition caused by mutations in TAP genes that impair the transport of cytosolic peptides to the ER, has been described both in mice [6] and humans [7]. This MHC class I immunodeficiency impairs the normal positive and negative selection in thymus and thus, a very limited functional $CD8^+$ T cell population is detected in both animals and patients. Strikingly, these individuals have no special predisposition to suffer viral infections or neoplasms, and only have a limited susceptibility to chronic respiratory bacterial infections. As cytolytic $CD8^+$ T lymphocytes are fundamental to control and eliminate both virus-infected and malignant cells, their ability to recognize TAP-independent ligands seems to help protect against viral infections and tumors in these immunocompromised individuals and animals.

Although TAP-independent viral epitopes were identified decades ago (reviewed in [3, 8, 9], very few studies have analyzed the cellular TAP-independent MHC class I peptidome [10-14]. In these studies, the cellular TAP-independent ligandome from immortalized cell lines has been defined using high-throughput immunopeptidomics

analyses. However, these tumor cell lines derived from immune cells have a dysregulated metabolism very different to the normal tissues. Therefore, using a similar high-throughput mass spectrometry analysis to that carried out with cell lines, we analyzed the TAP-independent MHC peptidome isolated from ex vivo spleen cells of TAP-deficient mice. In the current report, we identified 210 TAP-independent ligands bound to the H-2 K^b and D^b MHC class I molecules from spleens of TAP-deficient mice.

MATERIALS AND METHODS

Mice

TAP1-deficient B6.129S2-Tap1^{tm1Arp}/J mice [6] (stock no. 002944; The Jackson Laboratory, Bar Harbor, MN) were bred in our animal facilities in strict accordance with the recommendations of the Guide for the Care and Use of Laboratory Animals of the Spanish Comisión Nacional de Bioseguridad of the Ministerio de Medio Ambiente y Medio Rural y Marino (accreditation number 28079-34A). The protocol was approved by the Committee on Animal Experiment Ethics of the Institute of Health Carlos III (Permit Number: PI-283). Eight mice were analyzed as four biological replicates.

MHC class I-bound peptide isolation

The spleens from TAP-deficient mice were placed into a 40 µm cell strainer (Corning Inc., Corning, NY) and mashed using the plunger end of a syringe. After rinse with 5mL serum-free RPMI the stromal cells remain in the cell strainer. Supernatant was treated with Red Blood Cell Lysis Buffer Cocktail (Merck KGaA, Darmstadt, Germany) and splenocytes were recollected. The spleen cells were lysed in 1% CHAPS (Merck KGaA, Darmstadt, Germany), 20 mM Tris/HCl buffer, and 150 mM NaCl, pH 7.5 in the presence of the cOmplete™, Mini Protease Inhibitor Cocktail (Merck KGaA, Darmstadt, Germany). After centrifugation, the supernatant was passed first through a control precolumn containing CNBr-activated Sepharose 4B (GE Healthcare, Buckinghamshire, UK) to remove non-specific peptides and proteins. Next, the H-2 K^b/peptide or D^b/peptide complexes were isolated sequentially via affinity chromatography from the soluble cell extract fraction with Y3 [15] or 28-14-8s [16] monoclonal antibodies (mAbs), which are specific for monomorphic H-2 K^b or D^b determinants included in the alpha 1 and alpha 3 domains, respectively. A schematic representation of experimental design is shown in Figure 1. The MHC-bound peptides were eluted at 4ºC with 0.1% aqueous trifluoroacetic acid (TFA), separated from the

MHC molecules, and concentrated by ultra-filtration with a Vivaspin 2 filter, 5,000 MWCO HY (Sartorius Stedim Biotech, Goettingen, Germany), as previously described [17].

Electrospray-ion trap mass spectrometry analysis

Peptide mixtures recovered after the ultra-filtration step were desalted using OMIX Tips reversed-phase columns (C_{18}, 100 µl, Agilent Technologies, Santa Clara, CA) [17]. Each C_{18} tip was equilibrated with 50% acetonitrile in 0.1% TFA, washed with 0.1% TFA, and then loaded with the peptide mixture. The tip was then washed with an additional volume of 0.1% TFA, and the peptides were subsequently eluted with 50% acetonitrile in 0.1% TFA. Lastly, the peptide samples were concentrated to approximately 20 µl using vacuum centrifugation [17, 18 19].

The MHC class I peptides recovered from immunoprecipitated H-2 K^b or D^b-specific mAbs were analyzed by nanoLC-MS/MS using a Q-Exactive-Plus mass spectrometer fitted with an Ultimate 3000 RSLC nanocapillary UHPLC (Thermo Fisher Scientific, Waltham, MA), using the same parameters previously described [20]. The peptides were resolved on homemade Reprosil C18-Aqua capillary columns (75 micron ID, Dr. Maisch GmbH, Ammerbuch-Entringen, Germany) [21] with a 5-28% acetonitrile linear gradient for 2 h in the presence of 0.1% formic acid at a flow rate of 0.15 µL/min. The dynamic exclusion was set to 20 sec and the automatic gain control value for the full MS was set to $3x10^6$. The selected masses were fragmented from the survey scan of mass-to-charge ratio (m/z) 300-1,800 AMU at resolution 70,000. The 10 most intense masses were selected for fragmentation by higher-energy collisional dissociation (HCD) from each full mass spectrum. No fragmentation was performed for peptides with unassigned precursor ion charge states. MS/MS spectra were acquired with a resolution of 17,500 at m/z 200. The target value of the MS/MS was set to $1x10^5$ and the isolation window to 1.8 m/z. The maximum injection time was set to 100 ms

and normalized collision energy to 25 eV. The peptide match option was set to Preferred. Fragmented masses were dynamically excluded from further selection for fragmentation for 20 sec.

Database searches

Peptides were identified using the MaxQuant software tool [22] version 1.6.0.16 with the Andromeda search engine [23] using the mouse section of the UniProt/Swiss-Prot database (release 14.2.19, containing 54188 entries). Peptides were identified in the database assuming no specific enzyme proteolysis. Methionine oxidation and N-acetylation were accepted as variable modifications. The peptide precursors and fragment mass tolerances were set at 6 and 20 ppm, respectively. The identified peptides were selected when their score was > 40. The minimal peptide length was set to eight amino acid residues. The false discovery rate (FDR) was 0.01 for the peptide-spectrum matching. The LC-MS/MS data files of separate sets of immunoaffinity purified peptidomes and analyzed separately by LC-MS-MS were analyzed independently by the MaxQuant software to reduce misidentifications by the "match between runs" subroutine. The mass spectrometry data have been deposited to the MassIVE repository (https://massive.ucsd.edu) with the data set identifier MSV000083936.

In silico binding prediction of MHC class I ligands

The predicted binding of each peptide to MHC class I molecules was calculated using the artificial neural network-based alignment method NetMHCpan (version 4.0) (available in http://www.cbs.dtu.dk/services/NetMHCpan/).

Functional bioinformatics procedures

Functional annotation and biological term enrichment was performed using the Database for Annotation, Visualization and Integrated Discovery (DAVID;

https://david.ncifcrf.gov/). The protein-protein interaction network was visualized using the Search Tool for the Retrieval of Interacting Genes (STRING; https://string-db.org/).

Statistics

To analyze the statistical significance of the functional annotation and biological term enrichment analyses by DAVID the Benjamini-corrected modified Fisher Exact Test was utilized. To analyze the statistical significance of the protein-protein network analyses by STRING the protein-protein interaction enrichment p-value was considered.

RESULTS

Physiological processing generates multiple cellular ligands bound to murine MHC alleles in ex vivo spleen cells.

The H-2 K^b and D^b-bound peptide pools were isolated *ex vivo* from mouse primary spleen cells. These peptide mixtures were subsequently separated by capillary reversed-phase HPLC and were analyzed on-line using tandem mass spectrometry (Fig. 1). By means of bioinformatics tools over a mouse proteome database, different fragmentation spectra were resolved as peptidic sequences, derived from different mouse cellular proteins and bound to H-2 K^b or D^b (Table S1) class I molecules, respectively. None of the 210 fragmentation spectra from H-2 K^b and D^b-bound peptide pools were detect in the precolumn analysis confirming that the identified sequences were true MHC class I ligands.

Structural features of TAP-independent MHC class I ligands.

In TAP-sufficient cells H-2 K^b and D^b class I molecules usually bind peptides approximately 8-11 residues long (SYFPEITHI database: http://www.syfpeithi.de [24]). The size analysis indicated that 83% of the TAP-independent H-2 K^b ligands and 76% of the H-2 D^b ligands (Table S1) from TAP-deficient spleen cells are longer than those identified in TAP-sufficient cells. This increased peptide lengths was also described in TAP-independent ligands from mouse and human cell lines [11 12 25]. In addition, 18% of peptides derived from leader sequences and 14% from C-terminal end of parental proteins, similarly to TAP-independent ligandome from cell lines [11 12 25]. Also, nested set peptides with an identical core but with N- and/or C-extended residues from the same protein were identified among both H-2 K^b ligands and H-2 D^b ligands (Table S1), similarly as in the previously described TAP-independent ligandome from cell lines [11 12 25].

Next, prediction of the peptide binding of the TAP-independent ligands to each H-2 K^b and D^b class I molecule was analyzed. The theoretical affinity of the peptides from ex vivo spleen cells (Fig. 2) ranged in a similar way, and was not statistically significant, versus TAP-independent ligands from mouse and human cell lines [11 12 25].

Preferential biological processes of parental proteins from TAP-independent MHC class I ligands.

An assay comparing protein functions between the two different datasets (spleen and cell lines) from TAP-independent MHC class I ligands was conducted using gene ontology enrichment. Also, one study analyzing MHC class I ligands from TAP-sufficient spleen cells was included as control [26]. No biological processes were statistically significant associated with spleen ligandome from TAP-sufficient cells, consistent with the fact that the proteasome processes the whole proteome. In contrast, the source of TAP-independent ligands from ex vivo spleen cells was enriched mainly in genes involved in functions related with the immune system as expected from an organ with a high proportion of immune cells as B and T lymphocytes, macrophages and dendritic cells (Fig. 3). In contrast, several central biological processes associated with mRNA production, translation and expression, viral processes and other biological processes related with protein synthesis were linked to the ligandome from cell lines (Fig. 3), data that correlate with the immortal continuous origin of the virus-transformed cell lines utilized in previous studies [25].

Preferential location of parental proteins from TAP-independent MHC class I ligands.

Next, an assay comparing protein locations between the two different TAP-independent ligandomes (spleen and cell lines) and the control TAP-sufficient spleen peptidome was conducted using gene ontology enrichment. Newly, no specific cellular components were associated with the control peptidome, which correlates with the universal protein degradation activity previously described for the proteasome.

Moreover, multiple intracellular components as nuclear, nucleolus, cytoplasm, endoplasmic reticulum, Golgi apparatus or intracellular organelle were specifically associated with the TAP-independent ligandome from cell lines but not with the spleen cells (Fig. 4). In contrast, only two cellular components of the extracellular space were specifically associated with the TAP-independent ligandome from ex vivo spleen cells: “blood microparticle” and “extracellular space”, and not with their equivalent from cell lines (Fig. 4).

Functional protein association networks of parental proteins from TAP-independent MHC class I ligands.

In addition, an analysis of protein-protein interaction networks between both types of TAP-independent parental proteins (spleen and cell lines) was conducted using the STRING biological database. 392 protein-protein interactions were detected between the 174 parental proteins from TAP-independent spleen ligandome (Fig. 5). A significant proportion of these proteins had only one (16%) or no (33%) interactions with other TAP-deficient parental proteins (Fig. 5). In contrast, similar analysis with the 169 parental proteins from TAP-deficient cell lines ligandome showed 892 protein-protein interactions (Fig. 6), with an average node degree of 11.1 versus only 4.5 in the case of spleen ligandome. In addition, most of TAP-deficient parental proteins from cell lines were included in complex protein-protein networks, and only 25% of these proteins had only one or no interaction (Fig. 6).

Cleavage specificity of cellular proteases over TAP-independent MHC class I ligands.

To study the specificity of proteases involved in the generation of ligands in TAP-defective spleen cells, an analysis of residues on both sides of the hydrolyzed bonds of TAP-independent MHC class I ligands was carried out. No correlation was found when analyses of P_3, P_2, P'_1, P'_2, and P'_3 positions of scissile bonds were

performed. In contrast, two amino acids (Leu, and Phe) were increased in the P_1 positions of scissile bonds, which accounted for up to 10% of the total cleavages detected (Fig. 7, panel B). Both amino acids represent 32% of the total of cleaved residues, a very close number to 27% previously described for these two amino acids in the TAP-independent ligandome derived from cell lines [12]. In contrast the other two amino acids (Arg and Lys) also increased in the P_1 positions of scissile bonds in the TAP-independent ligandome from human cell lines, which accounted for other 30% of cleaved residues [12], were not significantly increased in the P_1 position of scissile bonds from TAP-independent spleen ligands.

DISCUSSION

The use of mass spectrometry analysis for identification of self-derived MHC ligands contributes to understand the mechanisms of antigen presentation that are associated with the cellular immune response. In these immunopeptidomics analyses immortalized cell lines were more commonly utilized. These tumor-derived cells lines have two main characteristics that condition the mass spectrometry analyses: a dysregulated metabolism, and a high expression of MHC class I molecules. Using a few billion cells, several thousand peptides bound to each individual MHC class I allele are identified in any immunopeptidomics analysis from TAP-sufficient cells. In contrast, only few tens or hundreds of MHC class I ligands have been described in the still very limited number of immunopeptidomics studies examining the TAP-independent ligandome of similar amounts of TAP-deficient cell lines [11] [12]. The MHC class I expression of mouse primary cells obtained from *ex vivo* tissues is one or two orders of magnitude lower than the cell lines. Thus, considering that the expression of H-2 D^b and K^b class I molecules from TAP-deficient mice spleen cells is about 20 and 200-fold lower than the respective spleen cells from TAP-sufficient cells, respectively [6], it is reasonable to assume an almost total absence of TAP-independent ligands in TAP-deficient spleen cells. Currently, using a sequential immunoprecipitation of MHC class I molecules, we identified 210 TAP-independent ligands that were processed and presented by the two class I molecules expressed in the spleen cells from TAP-deficient mice, a similar amount to HLA-A2 or -B27 TAP-independent ligandome previously described in human cell lines [12]). This *ex vivo* TAP-independent ligandome showed similar increased peptide lengths, presence of nested sets and low theoretical MHC binding affinity as the self-peptides obtained from TAP-deficient cell lines previously analyzed [11] [12]. These similar structural features of ligands from *in vitro* cultured cell lines and *ex vivo* physiological primary cells demonstrate that even in the complex and highly regulated physiological environment, where free peptides are

rapidly degraded to amino acids, peptides with low affinity can stabilize MHC class I molecules and be presented by these proteins. In the presence of TAP molecules, a high diversity of peptides is generated in the cytosol, a very degradative compartment for proteins with presence of multiple endopeptidases and exoproteases, and especially the proteasome. In these cells, the high affinity ligands are selected in their interaction with the MHC class I molecules [1]. In contrast, the lack of TAP severely decreases the contribution of the cytosol and thus, the few peptides generated by the more limited proteolytic activities from other less degradative compartments can bind to the high amounts of empty MHC class I molecules, although these are non-canonical peptides with a low affinity by the MHC class I molecule expressed in these TAP-deficient cells [11, 14, 12].

In contrast, four main differences were found at level of parental proteins from both TAP-independent MHC class I ligandomes. First, the proteins to yield TAP-independent antigen presentation from cell lines were associated with different central biological process of the dysregulated metabolism of these tumor-derived cells as mRNA and protein synthesis and regulation. Also viral processes were associated to these parental proteins, which could be related to the viral infection utilized to transform ex vivo immune cells into immortalized cell lines [27]. In contrast, the TAP-independent ligandome of ex vivo spleen cells was enriched almost exclusively in tissue-specific biological processes as those related with the immune system. It is striking that, although the immortalized cell lines previously utilized in these immunopeptidomics experiments also have an immune origin, nevertheless just one of 45 biological processes associated to parental proteins from these cell lines was related with the immune system. This indicates that the results with cell lines should be cautiously interpreted.

Second, although multiple cellular components were enriched in parental proteins of both TAP-independent ligandomes versus whole proteome a clear pattern

emerged when exclusive cellular components of each TAP-independent ligandome were analyzed. While different intracellular components were exclusively enriched in the TAP-independent ligandome from cell lines, only two components of the extracellular space were specifically enriched in the TAP-independent ligandome from ex vivo spleen cells: “blood microparticle” and “extracellular space”. Blood microparticles are microvesicles that circulate in the blood of healthy donors, but increased in different pathologies. These particles are produced by immune system cells, platelets or endothelial cells, and contain multiple proteins characteristic of the parental cell [28]. Of note, “extracellular space” component refers to everything outside the cell, but still within the organism excluding the extracellular matrix. Thus, our results indicate that the extracellular contribution is greater in ex vivo cells than in cultured cell lines and then, suggests that TAP-independent antigen presentation can be very dependent of the analyzed tissue.

Third, the analysis of protein-protein interaction networks between both types of TAP-independent parental proteins showed a higher functional association in cell lines than in ex vivo cells, indicating that the diversity of protein sources is increased in these spleen cells. These data correlate with the more physiological regulation in ex vivo cells, when no specific biological or functional processes are permanently activated.

And finally, a previous study showed that endoproteases, exhibiting specificity for Arg/Lys or Phe/Leu in the P_1 position of the scissile bond, were the main peptidases involved in the generation of ligandome from TAP-deficient cell lines [12]. However, in the ex vivo cells only the Phe/Leu cleavage specificity was detected with similar contribution as described in cell lines. Thus, in spleen cells a broad diversity of uncharacterized proteolytic activities would be involved in the MHC class I antigen processing of *in vivo* TAP-independent ligandome.

The global picture emerging from the current report shows that the low affinity TAP-independent ligandome from ex vivo spleen cells derives from a more diverse collection of endoprotease activities processing parental proteins with a lower functional interaction, and where the cell origin and the contribution of extracellular environment are more relevant than in cell lines. This indicates that future studies with different tissues and organs are needed to elucidate the diversity of MHC class I antigen presentation in TAP-deficient mice and humans.

FIGURES

Figure 1. Diagram of the scheme of sequential immunoprecipitation.

Spleen cells from TAP-deficient mice were lysed. MHC-peptide complexes were isolated via affinity chromatography of the soluble fraction of cell extracts with two mAbs, sequentially used as indicated in the Figure: Y3 (anti-H-2 K^b), and 28-14-8s (anti-H-2 D^b) after a precolumn used to remove non-specific binding proteins and peptides. The MHC class I molecules allotypes expressed in the TAP-deficient mice are indicated in a box.

Figure 2. Theoretical affinity of TAP-independent ligands from ex vivo spleen cells and mouse and human cell lines.

Box plots show the theoretical affinity of H-2 K^b and D^b class I ligands from TAP-deficient mouse spleen cells versus TAP-independent ligands from mouse H-2K^d [11] and human HLA-A2, -B27, -B51 and -C1 cell lines [12]. The theoretical affinities were calculated as percentile rank from the NetMHCpan server.

Figure 3. Functional annotation clustering of biological process of parental proteins from TAP-deficient splenocytes and cell lines.

Distribution of GO Biological Process categories exhibiting statistically significant differences between parental proteins from splenocytes and from cell lines with the whole proteome analyzed by DAVID bioinformatics tool. The statistical differences were calculated with Benjamini-corrected modified Fisher Exact Test.

Figure 4. Functional annotation clustering of cellular component of parental proteins from TAP-deficient splenocytes and cell lines.

Distribution of GO Cellular Component terms exhibiting statistically significant differences between parental proteins from splenocytes and from cell lines with the whole proteome calculated as in Figure 3.

Figure 5. Protein-protein network analysis of parental proteins from TAP-deficient splenocytes ligandome.

STRING analysis of parental proteins from TAP-deficient spleen cells ligands including predictions of protein interaction and association with experimentally determined interactions as follows: red line (indicates the presence of fusion evidence), green line (neighborhood evidence), blue line (co-occurrence evidence), purple line (experimental evidence), yellow line (text mining evidence), light blue line (database evidence, and black line (co-expression evidence). The protein-protein interaction enrichment p-value was $< 1x10^{-16}$.

Figure 6. Protein-protein network analysis of parental proteins from TAP-deficient cell lines ligandome.

STRING analysis of parental proteins from TAP-deficient cell lines ligands as in Figure 5. The protein-protein interaction enrichment p-value was $< 1x10^{-16}$.

Figure 7. Analysis of N- and C-end cleavage specificity in TAP-independent MHC class I ligands.

A diagram of residues involved in the generation of naturally processed MHC class I ligands by peptidase cleavages is shown in the upper panel. The distribution of P_1 amino acid residues of the scissile bonds created by peptidase cleavage is shown in the lower panel.

SUPPORTING INFORMATION:

The following supporting information is available free of charge at ACS website http://pubs.acs.org

Table S1. List of peptides identified using the MaxQuant software tool with the Andromeda search engine.

ACKNOWLEDGMENTS

This work was supported by the Spanish Ministry of Economy grants SAF2014-58052 and “Acción Estratégica en Salud” MPY 388/18 to D.L., and by Israel Science Foundation, grant No. 1435/16 to A. A. The funding agencies had no role in the study design, data collection, analysis decision to publish, or preparation of the manuscript. The authors had no conflicting financial interests.

BIBLIOGRAPHY

1. York, I. A., Goldberg, A. L., Mo, X. Y., and Rock, K. L. Proteolysis and class I major histocompatibility complex antigen presentation. *Immunol. Rev.* **1999**. 172: 49-66.

2. Jensen, P. E. Recent advances in antigen processing and presentation. *Nat. Immunol.* **2007**. 8: 1041-1048.

3. Oliveira, C. C. and van Hall, T. Alternative Antigen Processing for MHC Class I: Multiple Roads Lead to Rome. *Front Immunol.* **2015**. 6: 298.

4. Vigneron, N., Ferrari, V., Van den Eynde, B. J., Cresswell, P., and Leonhardt, R. M. Cytosolic Processing Governs TAP-Independent Presentation of a Critical Melanoma Antigen. *J. Immunol.* **2018**. 201: 1875-1888.

5. Doorduijn, E. M., Sluijter, M., Querido, B. J., Oliveira, C. C., Achour, A., Ossendorp, F., van der Burg, S. H., and van, H. T. TAP-independent self-peptides enhance T cell recognition of immune-escaped tumors. *J. Clin. Invest* **2016**. 126: 784-794.

6. van Kaer, L., Ashton Rickardt, P. G., Ploegh, H. L., and Tonegawa, S. TAP1 mutant mice are deficient in antigen presentation, surface class I molecules, and $CD4^{-}8^{+}$ T cells. *Cell* **1992**. 71: 1205-1214.

7. Cerundolo, V. and de la Salle, H. Description of HLA class I- and CD8-deficient patients: Insights into the function of cytotoxic T lymphocytes and NK cells in host defense. *Semin. Immunol.* **2006**. 18: 330-336.

8. Lopez, D., Lorente, E., Barriga, A., Johnstone, C., and Mir, C. Vaccination and the TAP-independent antigen processing pathways. *Expert. Rev. Vaccines.* **2013**. 12: 1077-1083.

9. Del Val, M., Lazaro, S., Ramos, M., and Antón, L. C. Are membrane proteins favored over cytosolic proteins in TAP-independent processing pathways? *Mol. Immunol.* **2013**. 55: 117-119.

10. Weinzierl, A. O., Rudolf, D., Hillen, N., Tenzer, S., van Endert, P., Schild, H., Rammensee, H. G., and Stevanovic, S. Features of TAP-independent MHC class I ligands revealed by quantitative mass spectrometry. *Eur J Immunol.* **2008**. 38: 1503-1510.

11. Suri, A., Walters, J. J., Levisetti, M. G., Gross, M. L., and Unanue, E. R. Identification of naturally processed peptides bound to the class I MHC molecule $H\text{-}2K^{d}$ of normal and TAP-deficient cells. *Eur. J. Immunol.* **2006**. 36: 544-557.

12. Lorente, E., Infantes, S., Barnea, E., Beer, I., Barriga, A., Garcia-Medel, N., Lasala, F., Jimenez, M., Admon, A., and Lopez, D. Diversity of natural self-derived ligands presented by different HLA class I molecules in transporter antigen processing-deficient cells. *PLoS. ONE.* **2013**. 8: e59118.

13. Oliveira, C. C., van Veelen, P. A., Querido, B., de Ru, A., Sluijter, M., Laban, S., van der Burg, S. H., Offringa, R., and van Hall, T. The nonpolymorphic MHC Qa-

1b mediates CD8+ T cell surveillance of antigen-processing defects. *J Exp. Med* **2009**. 207: 207-221.

14. Lampen, M. H., Hassan, C., Sluijter, M., Geluk, A., Dijkman, K., Tjon, J. M., de Ru, A. H., van der Burg, S. H., van Veelen, P. A., and van, H. T. Alternative peptide repertoire of HLA-E reveals a binding motif that is strikingly similar to HLA-A2. *Mol. Immunol.* **2013**. 53: 126-131.

15. Hammerling, G. J., Rusch, E., Tada, N., Kimura, S., and Hammerling, U. Localization of allodeterminants on H-2Kb antigens determined with monoclonal antibodies and H-2 mutant mice. *Proc. Natl. Acad. Sci. U. S. A* **1982**. 79: 4737-4741.

16. Allen, H., Wraith, D., Pala, P., Askonas, B., and Flavell, R. A. Domain interactions of H-2 class I antigens alter cytotoxic T-cell recognition sites. *Nature* **1984**. 309: 279-281.

17. Johnstone, C., Lorente, E., Barriga, A., Barnea, E., Infantes, S., Lemonnier, F. A., David, C. S., Admon, A., and Lopez, D. The Viral Transcription Group Determines the HLA Class I Cellular Immune Response Against Human Respiratory Syncytial Virus. *Mol. Cell Proteomics.* **2015**. 14: 893-904.

18. Lorente, E., Infantes, S., Barnea, E., Beer, I., Garcia, R., Lasala, F., Jimenez, M., Vilches, C., Lemonnier, F. A., Admon, A., and López, D. Multiple viral ligands naturally presented by different class I molecules in transporter antigen processing-deficient vaccinia virus-infected cells. *J Virol* **2012**. 86: 527-541.

19. Lorente, E., Infantes, S., Abia, D., Barnea, E., Beer, I., Garcia, R., Lasala, F., Jimenez, M., Mir, C., Morreale, A., Admon, A., and Lopez, D. A Viral, Transporter Associated with Antigen Processing (TAP)-independent, High Affinity Ligand with Alternative Interactions Endogenously Presented by the Nonclassical Human Leukocyte Antigen E Class I Molecule. *J. Biol. Chem.* **2012**. 287: 34895-34903.

20. Barnea, E., Melamed, K. D., Haimovich, Y., Satumtira, N., Dorris, M. L., Nguyen, M. T., Hammer, R. E., Tran, T. M., Colbert, R. A., Taurog, J. D., and Admon, A. The Human Leukocyte Antigen (HLA)-B27 Peptidome in Vivo, in Spondyloarthritis-susceptible HLA-B27 Transgenic Rats and the Effect of Erap1 Deletion. *Mol. Cell Proteomics.* **2017**. 16: 642-662.

21. Ishihama, Y., Rappsilber, J., Andersen, J. S., and Mann, M. Microcolumns with self-assembled particle frits for proteomics. *J Chromatogr. A* **2002**. 979: 233-239.

22. Cox, J. and Mann, M. MaxQuant enables high peptide identification rates, individualized p.p.b.-range mass accuracies and proteome-wide protein quantification. *Nat. Biotechnol.* **2008**. 26: 1367-1372.

23. Cox, J., Neuhauser, N., Michalski, A., Scheltema, R. A., Olsen, J. V., and Mann, M. Andromeda: a peptide search engine integrated into the MaxQuant environment. *J. Proteome. Res.* **2011**. 10: 1794-1805.

24. Rammensee, H. G., Bachmann, J., Emmerich, N. P. N., Bachor, O. A., and Stevanovic, S. SYFPEITHI: database for MHC ligands and peptide motifs. *Immunogenetics* **1999**. 50: 213-219.

25. Martin-Galiano, A. J. and Lopez, D. Computational characterization of the peptidome in transporter associated with antigen processing (TAP)-deficient cells. *PLoS. ONE.* **2019**. 14: e0210583.

26. Schuster, H., Shao, W., Weiss, T., Pedrioli, P. G. A., Roth, P., Weller, M., Campbell, D. S., Deutsch, E. W., Moritz, R. L., Planz, O., Rammensee, H. G., Aebersold, R., and Caron, E. A tissue-based draft map of the murine MHC class I immunopeptidome. *Sci. Data* **2018**. 5: 180157.

27. Sie, L., Loong, S., and Tan, E. K. Utility of lymphoblastoid cell lines. *J. Neurosci. Res.* **2009**. 87: 1953-1959.

28. Simak, J. and Gelderman, M. P. Cell membrane microparticles in blood and blood products: potentially pathogenic agents and diagnostic markers. *Transfus. Med. Rev.* **2006**. 20: 1-26.

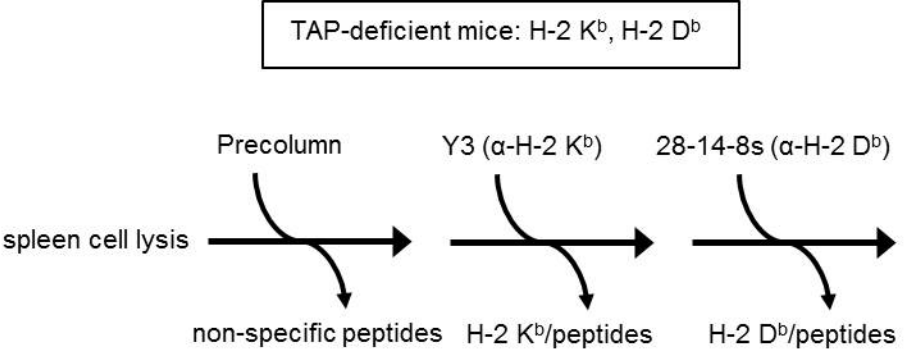
TAP-deficient mice: H-2 Kb, H-2 Db
Precolumn
Y3 (α-H-2 Kb)
28-14-8s (α-H-2 Db)
spleen cell lysis
non-specific peptides
H-2 Kb/peptides
H-2 Db/peptides

Figure 1

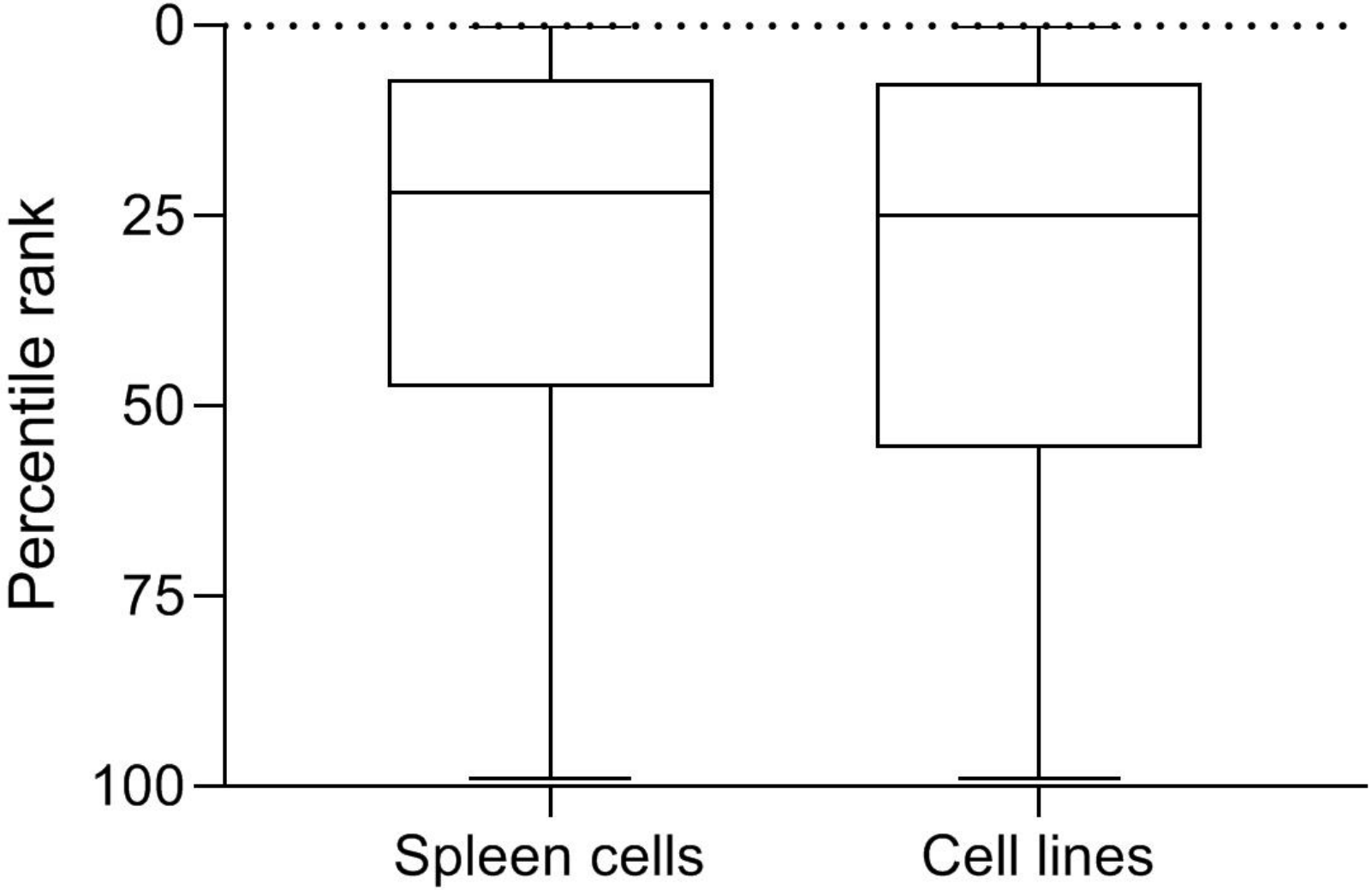

Figure 2

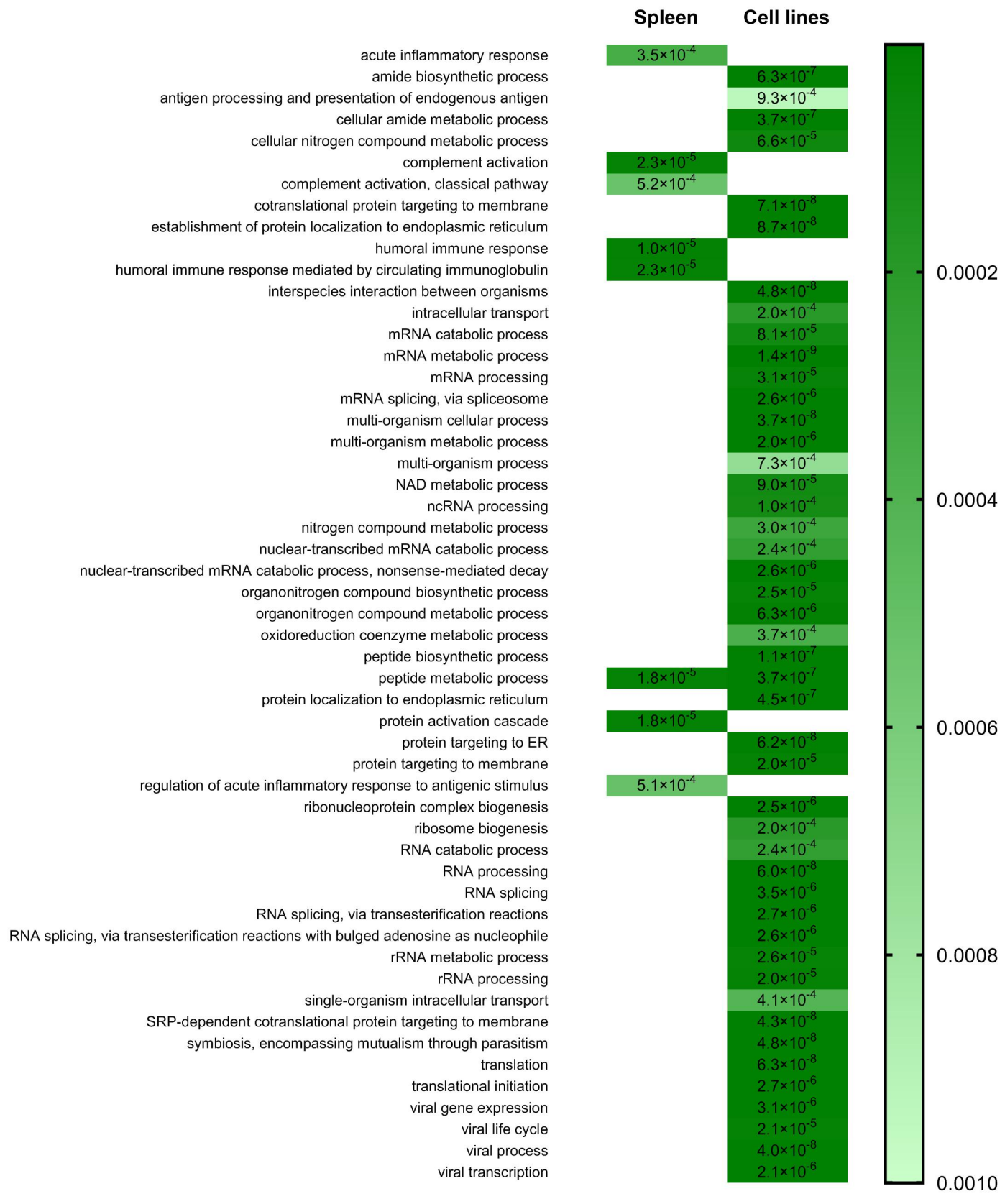
Biological processes
Spleen
Cell lines
acute inflammatory response
amide biosynthetic process
antigen processing and presentation of endogenous antigen
cellular amide metabolic process
cellular nitrogen compound metabolic process
complement activation
complement activation, classical pathway
cotranslational protein targeting to membrane
establishment of protein localization to endoplasmic reticulum
humoral immune response
humoral immune response mediated by circulating immunoglobulin
interspecies interaction between organisms
intracellular transport
mRNA catabolic process
mRNA metabolic process
mRNA processing
mRNA splicing, via spliceosome
multi-organism cellular process
multi-organism metabolic process
multi-organism process
NAD metabolic process
ncRNA processing
nitrogen compound metabolic process
nuclear-transcribed mRNA catabolic process
nuclear-transcribed mRNA catabolic process, nonsense-mediated decay
organonitrogen compound biosynthetic process
organonitrogen compound metabolic process
oxidoreduction coenzyme metabolic process
peptide biosynthetic process
peptide metabolic process
protein localization to endoplasmic reticulum
protein activation cascade
protein targeting to ER
protein targeting to membrane
regulation of acute inflammatory response to antigenic stimulus
ribonucleoprotein complex biogenesis
ribosome biogenesis
RNA catabolic process
RNA processing
RNA splicing
RNA splicing, via transesterification reactions
RNA splicing, via transesterification reactions with bulged adenosine as nucleophile
rRNA metabolic process
rRNA processing
single-organism intracellular transport
SRP-dependent cotranslational protein targeting to membrane
symbiosis, encompassing mutualism through parasitism
translation
translational initiation
viral gene expression
viral life cycle
viral process
viral transcription
3.5×10-4
2.3×10-5
5.2×10-4
1.0×10-5
2.3×10-5
1.8×10-5
1.8×10-5
5.1×10-4
6.3×10-7
9.3×10-4
3.7×10-7
6.6×10-5
7.1×10-8
8.7×10-8
4.8×10-8
2.0×10-4
8.1×10-5
1.4×10-9
3.1×10-5
2.6×10-6
3.7×10-8
2.0×10-6
7.3×10-4
9.0×10-5
1.0×10-4
3.0×10-4
2.4×10-4
2.6×10-6
2.5×10-5
6.3×10-6
3.7×10-4
1.1×10-7
3.7×10-7
4.5×10-7
6.2×10-8
2.0×10-5
2.5×10-6
2.0×10-4
2.4×10-4
6.0×10-8
3.5×10-6
2.7×10-6
2.6×10-6
2.6×10-5
2.0×10-5
4.1×10-4
4.3×10-8
4.8×10-8
6.3×10-8
2.7×10-6
3.1×10-6
2.1×10-5
4.0×10-8
2.1×10-6
0.0002
0.0004
0.0006
0.0008
0.0010

Figure 3

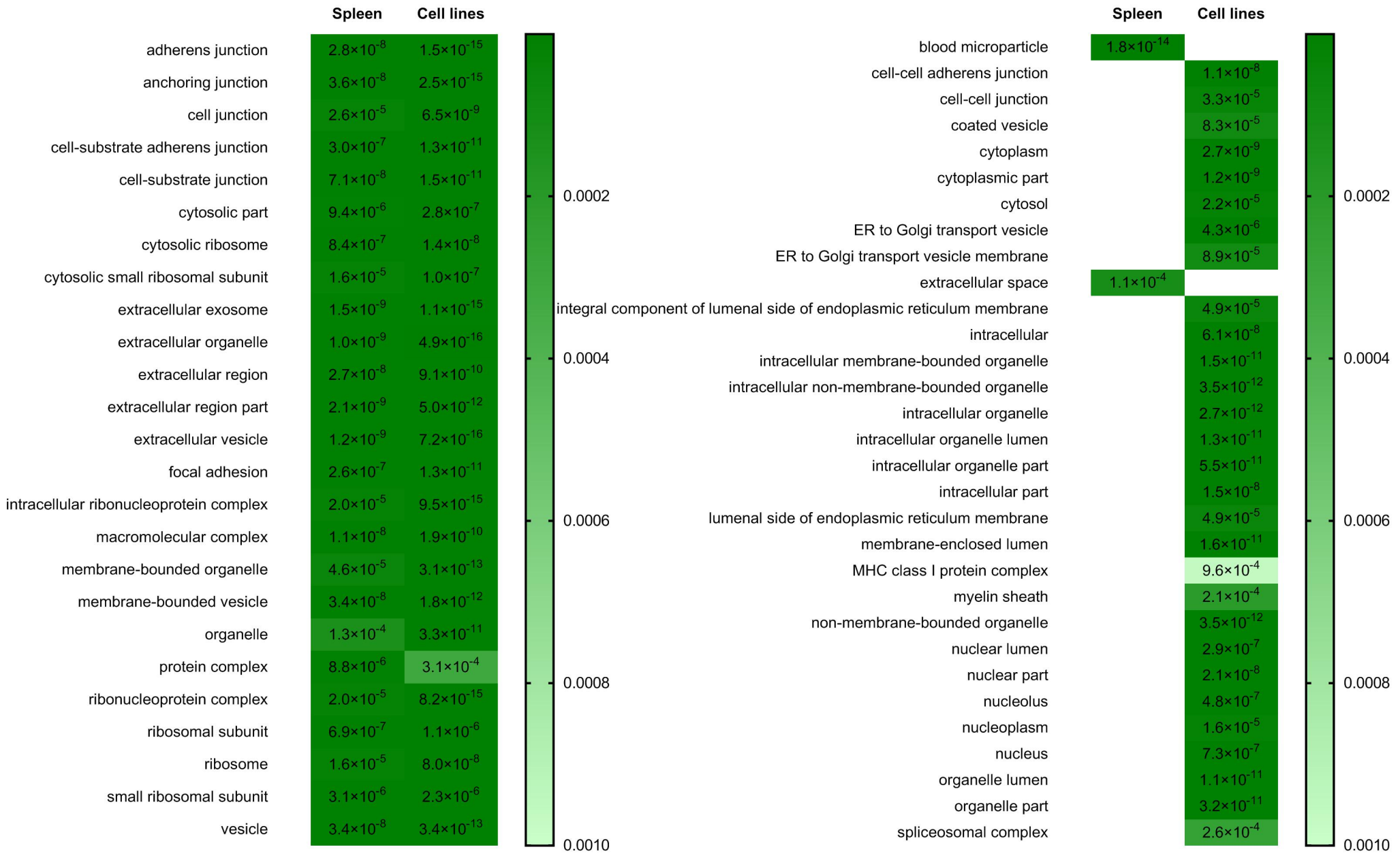
Cellular components
Spleen
Cell lines
adherens junction 2.8×10-8 1.5×10-15
anchoring junction 3.6×10-8 2.5×10-15
cell junction 2.6×10-5 6.5×10-9
cell-substrate adherens junction 3.0×10-7 1.3×10-11
cell-substrate junction 7.1×10-8 1.5×10-11
cytosolic part 9.4×10-6 2.8×10-7
cytosolic ribosome 8.4×10-7 1.4×10-8
cytosolic small ribosomal subunit 1.6×10-5 1.0×10-7
extracellular exosome 1.5×10-9 1.1×10-15
extracellular organelle 1.0×10-9 4.9×10-16
extracellular region 2.7×10-8 9.1×10-10
extracellular region part 2.1×10-9 5.0×10-12
extracellular vesicle 1.2×10-9 7.2×10-16
focal adhesion 2.6×10-7 1.3×10-11
intracellular ribonucleoprotein complex 2.0×10-5 9.5×10-15
macromolecular complex 1.1×10-8 1.9×10-10
membrane-bounded organelle 4.6×10-5 3.1×10-13
membrane-bounded vesicle 3.4×10-8 1.8×10-12
organelle 1.3×10-4 3.3×10-11
protein complex 8.8×10-6 3.1×10-4
ribonucleoprotein complex 2.0×10-5 8.2×10-15
ribosomal subunit 6.9×10-7 1.1×10-6
ribosome 1.6×10-5 8.0×10-8
small ribosomal subunit 3.1×10-6 2.3×10-6
vesicle 3.4×10-8 3.4×10-13
0.0002
0.0004
0.0006
0.0008
0.0010
Spleen
Cell lines
blood microparticle 1.8×10-14
cell-cell adherens junction 1.1×10-8
cell-cell junction 3.3×10-5
coated vesicle 8.3×10-5
cytoplasm 2.7×10-9
cytoplasmic part 1.2×10-9
cytosol 2.2×10-5
ER to Golgi transport vesicle 4.3×10-6
ER to Golgi transport vesicle membrane 8.9×10-5
extracellular space 1.1×10-4
integral component of lumenal side of endoplasmic reticulum membrane 4.9×10-5
intracellular 6.1×10-8
intracellular membrane-bounded organelle 1.5×10-11
intracellular non-membrane-bounded organelle 3.5×10-12
intracellular organelle 2.7×10-12
intracellular organelle lumen 1.3×10-11
intracellular organelle part 5.5×10-11
intracellular part 1.5×10-8
lumenal side of endoplasmic reticulum membrane 4.9×10-5
membrane-enclosed lumen 1.6×10-11
MHC class I protein complex 9.6×10-4
myelin sheath 2.1×10-4
non-membrane-bounded organelle 3.5×10-12
nuclear lumen 2.9×10-7
nuclear part 2.1×10-8
nucleolus 4.8×10-7
nucleoplasm 1.6×10-5
nucleus 7.3×10-7
organelle lumen 1.1×10-11
organelle part 3.2×10-11
spliceosomal complex 2.6×10-4
0.0002
0.0004
0.0006
0.0008
0.0010

Figure 4

Spleen cells

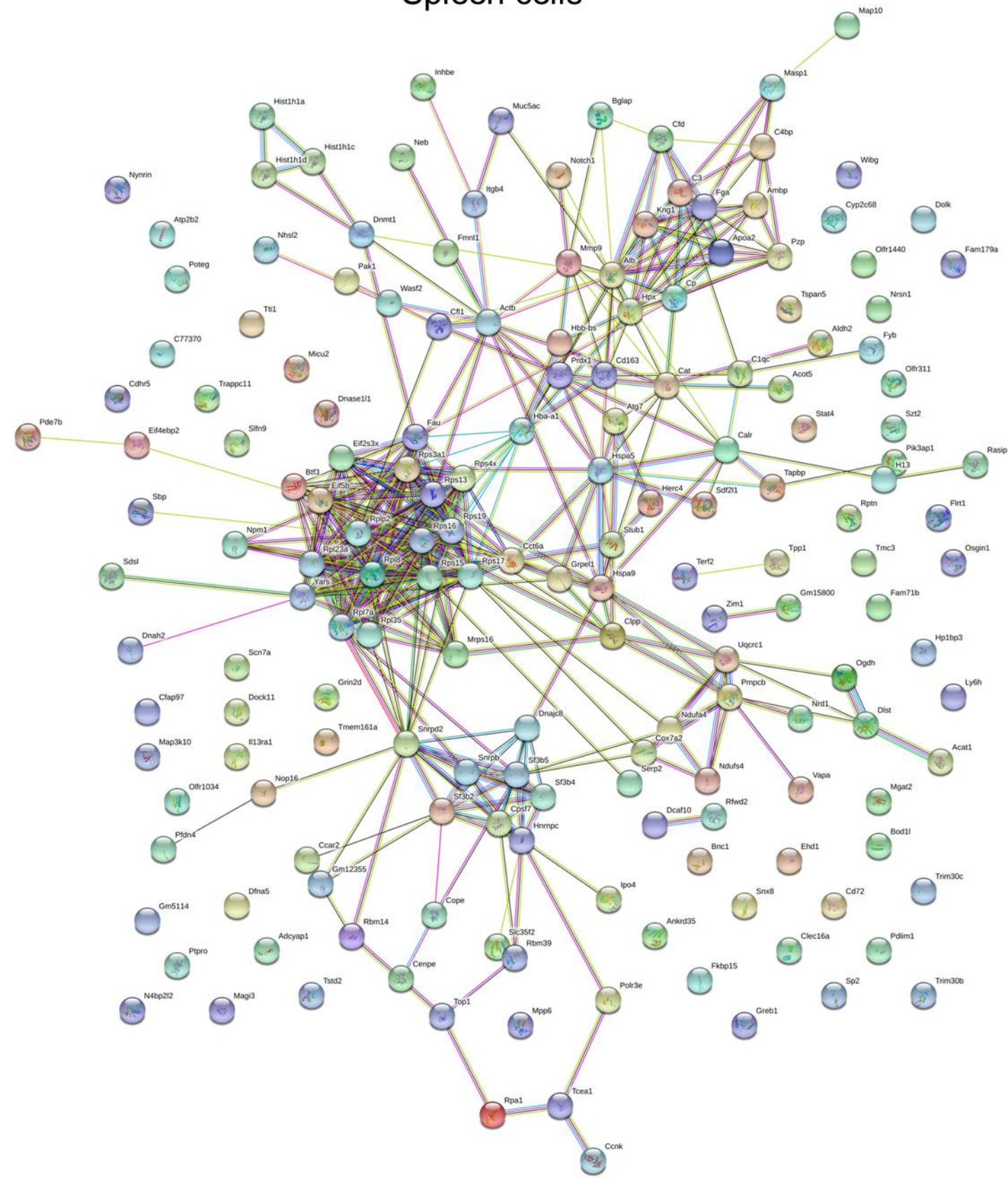

Figure 5

Cell lines

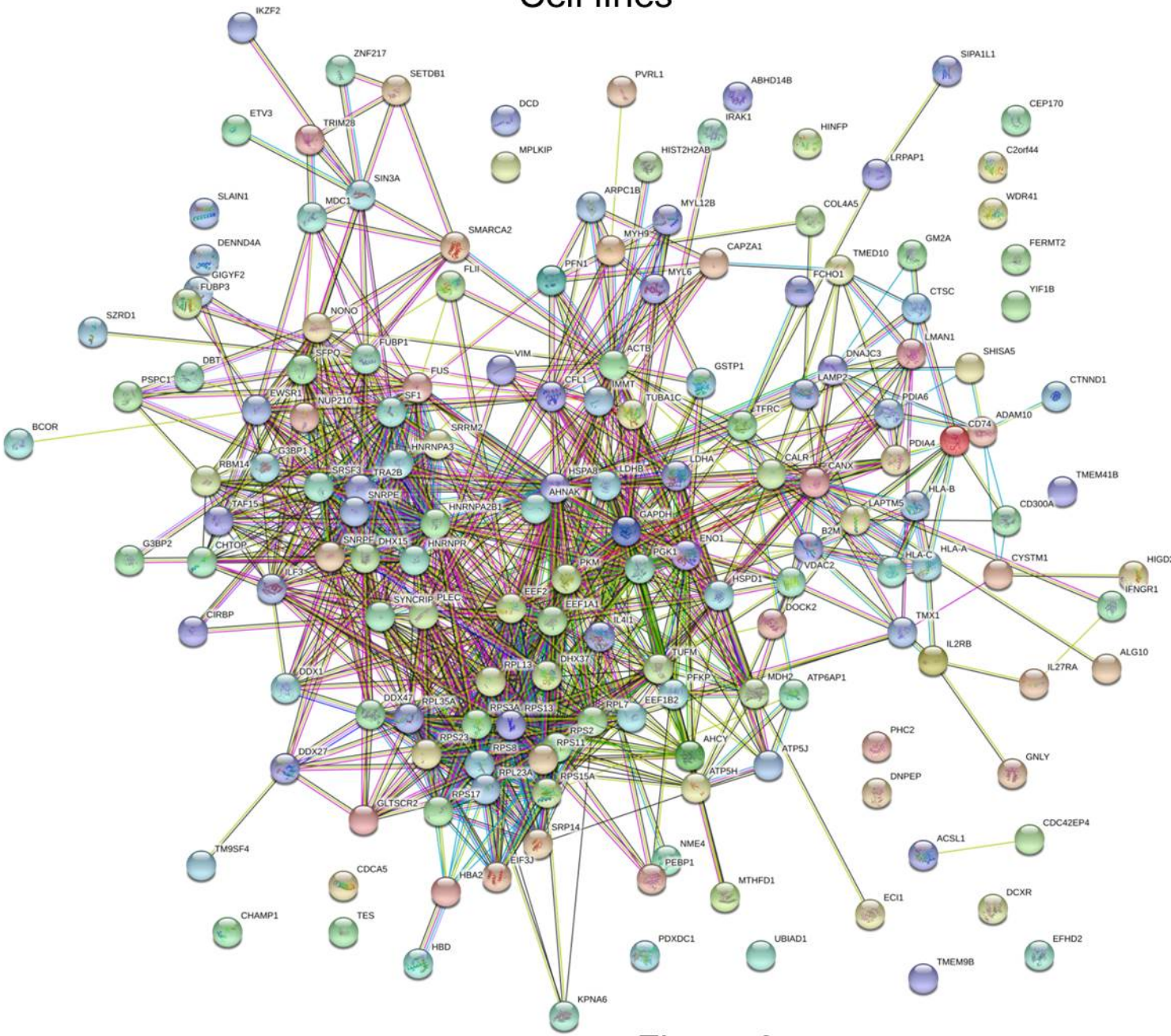

Figure 6

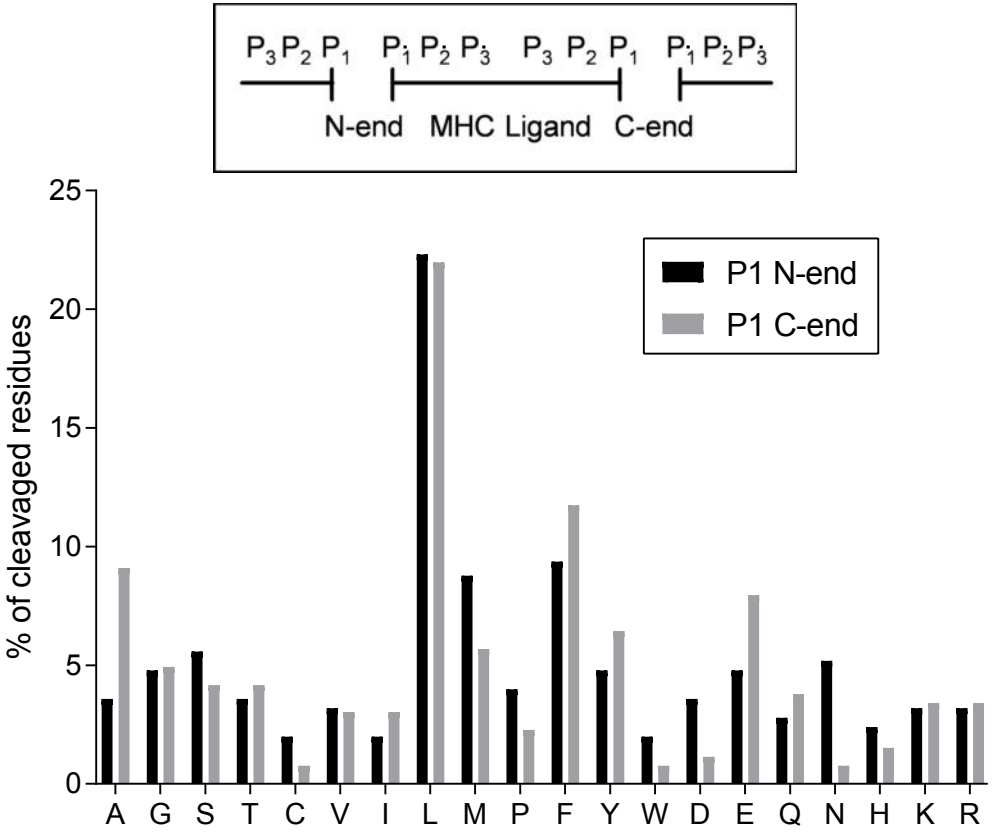
P3 P2 P1
P1 P2 P3
P3 P2 P1
P1 P2 P3
N-end
MHC Ligand
C-end
P1 N-end
P1 C-end
% of cleavaged residues
25
20
15
10
5
0
A G S T C V I L M P F Y W D E Q N H K R

Figure 7